Two-photon ionization of xenon at 193 nm

A. W. McCown, M. N. Ediger, and J. G. Eden
Department of Electrical Engineering, University of Illinois, Urbana, Illinois 61801
(Received 24 June 1982)

A microwave bridge has been used in conjunction with an ArF excimer laser to measure the coefficient α for two-photon ionization of Xe at 193 nm. The bridge permits the measurement of ν_m, the collision frequency for momentum transfer, and the display of the temporal history of the absolute electron density. Although considerably larger than previous estimates, the value of α reported here (4×10^{-32} cm^{4}W^{-1}) is in agreement with the recent theoretical calculations of McGuire.

I. INTRODUCTION

The multiphoton ionization (MPI) of xenon using a laser was first demonstrated by Voronov and Delone[1] (ruby—0.694 μm) and Barhudarova *et al.*[2] (Nd:YAG—1.064 μm). Later, Agostini and co-workers[3] and Lompre *et al.*[4] showed that the non-resonant photoionization process is governed by the power-law intensity dependence, I^N (where N is the minimum number of photons necessary to ionize the atom), that is predicted by perturbation theory. Since 1966, considerable effort has been devoted to studying the MPI of the rare gases and xenon, in particular.[5–7] In the last three years, three-, four-, five-, and six-photon ionization of Xe, involving lasers operating near 250, 351, 425, and 532 nm, respectively, has been observed.[7–10]

With the recent advent of the ArF laser came the capability of ionizing Xe with two photons. Bischel and co-workers[11] have exploited this tool to investigate the gas-phase formation kinetics of XeF and XeO and have estimated the two-photon coefficient α for Xe at 193 nm to be 1×10^{-34} cm^4 W^{-1}. Subsequently, Hodges, Lee, and Moseley[12] experimen-

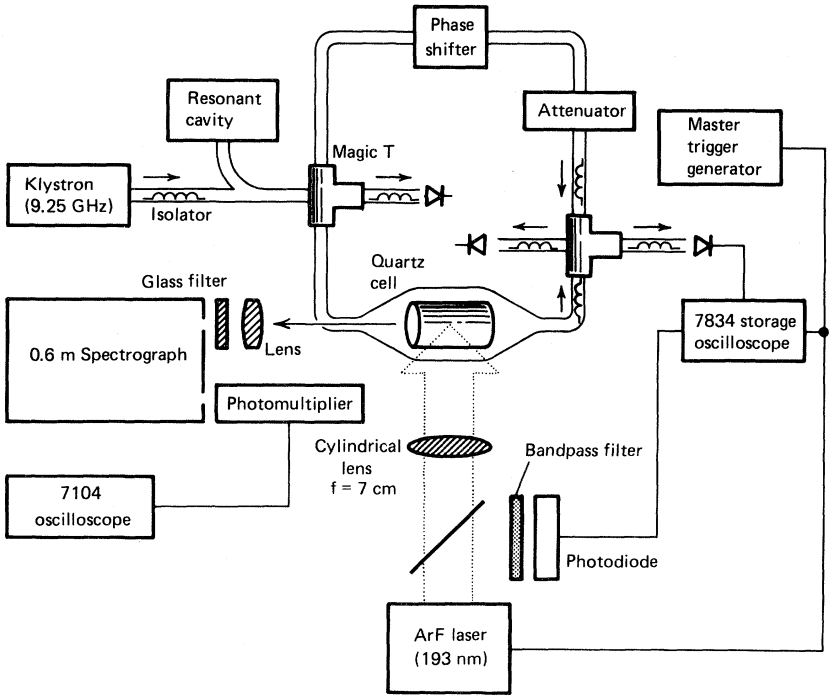

FIG. 1. Schematic diagram of the experimental apparatus. The diameter of the cylindrical waveguide has been exaggerated for clarity. For studies of the temporal history of the Xe* 828.0-nm fluorescence, the spectrograph was replaced by a photomultiplier with a GaAs photocathode and a dielectric bandpass filter.

tally determined the lower limit for α to be 5×10^{-34} cm^4 W^{-1}.

The determination of α at 193 nm using a microwave bridge technique to measure the absolute photoelectron density is reported here. Although roughly two orders of magnitude larger than the previously published results mentioned above, the value of α measured in these experiments (4×10^{-32} cm^4 W^{-1}) is in agreement with the calculations recently published by McGuire.[13]

II. EXPERIMENTAL APPARATUS AND THEORETICAL BASIS FOR THE MICROWAVE MEASUREMENTS

Aside from the microwave bridge used in detecting photoelectrons, the experimental apparatus illustrated in Fig. 1 is similar to that generally used in multiphoton ionization studies. The output of an ArF laser [linewidth = 5.2 Å or $\sim$ 140-cm^{-1} full width at half maximum (FWHM); beam randomly polarized] was focused to a line coinciding with the axis of a quartz tube using a 7-cm focal length cylindrical lens. By inserting several quartz flats in the optical path, the laser energy per pulse incident on the cell was varied from 25 to 175 mJ [or $\sim$20 to 146 MW cm^{-2} (at the focus) in a 13 ns FWHM pulse]. An S-20 surface, vacuum photodiode, and a bandpass filter monitored the time dependence of the ArF laser intensity. The photodiode was calibrated against a Gen-Tec pyroelectric detector and a Scientech energy meter and corrections to the laser intensity were made for the transmission of the lens (93%) and the cell wall (91%).

The Xe-containing cells were constructed of 20-mm inner diameter suprasil quartz and are 6.5 cm in length. After being evacuated to $<1\times10^{-7}$ Torr and flamed (under vacuum) with a hydrogen torch to degas the walls, each tube was backfilled with 1–500 Torr of research grade Xe and sealed off. The xenon was condensed by immersing the cells in liquid N_2 and a barium getter was flashed to further purify the gas. A separate quartz cell was prepared for each xenon pressure studied.

The gas cell was placed within a 15-cm section of cylindrical waveguide (slotted to permit the entrance of the ArF beam) which was situated in one arm of a microwave bridge. The cylindrical waveguide was matched to the bridge (constructed of rectangular WR-90 guide) by two tapered sections.

A. Operation of the microwave bridge

The output of a klystron at 9.252 GHz was split into two parts by a magic-T and one component impinged on the optical cell. The other portion of the microwave signal passed through the reference arm of the bridge which contained a phase shifter and attenuator. The signals in both arms of the bridge were added by a second magic-T and the sum was detected by an output diode. Before the laser was fired, the bridge was balanced or "nulled" by adjusting the phase and attenuation in the reference arm to exactly compensate for the insertion loss due to the optical cell. The creation of Xe photoelectrons by the 193-nm laser unbalanced the bridge and led to the appearance of a time-varying signal at the output diode.

An arbitrary phase shift $\Delta\theta$ was then introduced. With the firing of the ArF laser, a time-varying phase was produced which opposed $\Delta\theta$ and arose from the photoelectron density. For a particular value of electron density, then, the phase shift introduced by the plasma exactly equaled $\Delta\theta$, the bridge was momentarily balanced and a minimum (but nonzero value) in the signal was observed at the output diode. The minimum generally occurred twice in the life of the plasma (i.e., for each laser shot)—once when the electron density climbed past this critical density (n_c) and again as n fell below it. Therefore, for a given laser intensity (and peak electron density) and $\Delta\theta$, the attenuation in the reference arm was adjusted until the minimum in the output signal went to zero. In this way, ordered pairs of $\Delta\theta$ and attenuation were determined for a specific Xe pressure and, as shown below, were used to determine the collision frequency for momentum transfer, ν_m.

B. Theoretical relations for ω_p and ν_m

The expression for the propagation constant of an electromagnetic wave traveling along a waveguide that is partially filled with a conducting medium is

$$\gamma^2-\gamma_0^2=j\omega\mu_0\frac{\int\int\int\vec{E}_0\cdot\vec{J}\,dV}{\int\int\int\vec{E}_0\cdot\vec{E}\,dV}\,, \tag{1}$$

where γ_0 and $\vec{E}_0$ are the propagation constant and electric field, respectively, for the evacuated waveguide, $\vec{E}$ is the electric field in the presence of the plasma and ω is the radian frequency of the probing microwave field (5.8×10^{10} s^{-1}). For a plasma dielectric, the complex propagation constant γ is

$$\gamma=\alpha+i\beta\,,$$

where α (not to be confused with the two-photon ionization coefficient) and β are the attenuation and

phase coefficients, respectively, for the microwave signal propagating through the plasma.

Rewriting $\vec{J}$ in terms of the complex conductivity σ and separating the real and imaginary parts of Eq. (1), then

$$(\alpha^2-\beta^2)+\beta_0^2=\frac{\omega^2}{c^2}\frac{e^2}{m\epsilon_0}\frac{1}{\nu_m^2+\omega^2}\frac{\int\int\int nE_0^2dV}{\int\int\int E_0^2dV} \tag{2}$$

and

$$2\alpha\beta=\frac{\omega^2}{c^2}\frac{e^2}{m\epsilon_0}\frac{\nu_m}{\omega}\frac{1}{\nu_m^2+\omega^2}\frac{\int\int\int nE_0^2dV}{\int\int\int E_0^2dV}\ , \tag{3}$$

where $\vec{E}\approx\vec{E}_0$.

However, the electron density n is a function of position within the cell. That is,

$$n=n_pf(r,\phi,z)\ ,$$

where n_p is the peak (axial) electron density and f is expressed in terms of cylindrical coordinates. Also, the phase coefficient β is related to the experimentally determined phase shift $\Delta\theta$ by the relation

$$\Delta\theta=(\beta_0-\beta)L\ ,$$

where, for a cylindrical waveguide of radius a,

$$\beta_0=\left[\frac{\omega^2}{c^2}-\left[\frac{1.84}{a}\right]^2\right]^{1/2}$$

and L is the width of the focused laser beam (2.9 cm). Consequently, Eqs. (2) and (3) can be solved for the plasma frequency ω_p and ν_m (in this case, for electrons in Xe):

$$\omega_p^2=\frac{n_pe^2}{m\epsilon_0}=F^{-1}(\nu_m^2+\omega^2)\times\left\{1-\frac{c^2}{\omega^2}\left[\left[\frac{1.84}{a}\right]^2+\beta^2-\alpha^2\right]\right\} \tag{4}$$

and

$$\nu_m=\frac{2\alpha\beta\omega}{\frac{\omega^2}{c^2}-\left[\left[\frac{1.84}{a}\right]^2+\beta^2-\alpha^2\right]}\ , \tag{5}$$

where

$$F=\frac{\int\int\int fE_0^2dV}{\int\int\int E_0^2dV}\ , \tag{6}$$

$a=1.27$ cm, and m is the rest mass of an electron.

It should be noted here that, except for the "filling factor" F in Eq. (4), Eqs. (4) and (5) are identical to those for uniformly filled waveguides.

Evaluating F [Eq. (6)] required detailed measurements of the laser-beam contour and knowledge of the microwave field present in the cylindrical waveguide. The profile of the laser beam was determined by recording burn patterns every 0.6 mm and measuring the beam cross section with a comparator. At the lens focus, the cross section was found to be 0.02×2.9 cm^2. Also, the beam height h is symmetrical about the focus, and for a fixed beam width (2.9 cm), the laser intensity varies inversely with h. From these measurements, therefore, it was found that the electron density at any point along the focused beam can be expressed analytically in terms of the peak ($x=0$, where x is the r coordinate for $\phi=0$) value as

$$\frac{n}{n_p}=(1+30.7x^2)^{-1},\quad 0\le x\le 1 \tag{7}$$

where x is expressed in cm.

This relationship is consistent with the quadratic dependence of electron density on intensity and the linear growth of the beam height away from the focus. In any case, f is simply the right-hand side of Eq. (7).

Secondly, the dominant field mode in the cylindrical guide is TE_{11} whose electric field has the form

$$\vec{E}_0=2E_1\left[\frac{J_1(kr)}{kr}\cos\phi\hat{r}-\left[J_0(kr)-\frac{J_1(kr)}{kr}\right]\sin\phi\hat{\phi}\right]\ , \tag{8}$$

where ϕ is the azimuthal angle in the cylindrical coordinate system (i.e., $dV=r\,dr\,d\phi\,dz$), J_0 and J_1 are the zeroth- and first-order Bessel functions, respectively, and the factor of 2 is dictated by the constraint that $|\vec{E}_0|=E_1$ at $r=0$. The Bessel functions in (8) were expanded in power series and the first four terms were retained. Owing to the tight focusing of the laser beam, the magnitude of h (even at the cell walls) is $\ll a$ and so $\cos\phi\simeq1$ and $\sin\phi\simeq0$ (i.e., azimuthal component of $\vec{E}$ in the vicinity of the ArF beam is negligible). Substituting (7) and the expansion of (8) into (6) and now letting $dV=h\,dx\,dz$, F was determined to be $\frac{1}{150}$.

Therefore, the nonuniformity of the electric field and photoelectron density in the cell have been accounted for and ω_p and ν_m are expressed entirely in terms of the experimentally measured phase shift and attenuation coefficients. Also, this analysis

need not be repeated for different gases.

With the use of the microwave bridge and Eq. (5), ν_m was measured (over several trials) at 300-Torr Xe to be $(3.9\pm1.0)\times10^{10}$ s^{-1} or $(4.0\pm1.0)\times10^{-9}$ cm^3 s^{-1}. Remembering that the difference in energy between two ArF photons ($103\,466\pm70$ cm^{-1}) and the $^2P_{3/2}$ level of the Xe^+ ion ground state ($97\,834$ cm^{-1}) is approximately 0.7 eV, then this value of ν_m is in rough agreement with the data of Frost and Phelps[14] who find $\nu_m \simeq 6\times10^{-9}$ $cm^3 s^{-1}$ for 0.7-eV electrons. It should be emphasized, however, that Frost and Phelps's momentum-transfer cross sections were calculated from electron drift velocity measurements whereas in this work, ν_m is evaluated from the ac conductivity of the plasma. Thus, the comparison between the two values must be viewed as order-of-magnitude agreement.

Finally, it is evident from Eqs. (4) and (5) that ω_p can be expressed entirely in terms of ν_m and α. Therefore, once ν_m was known, the reference arm of the bridge was no longer necessary and so for a particular Xe pressure and ArF intensity I only single-pass attenuation coefficients were measured for the remainder of the experiments.

C. Fluorescence measurements

In addition to absolute electron-density measurements, the axial fluorescence due to the Xe $6p[\frac{1}{2}]_0 \rightarrow 6s[\frac{3}{2}]_1$ transition at 828.0 nm was viewed through a 6-mm diameter hole drilled in a waveguide elbow (E-plane bend). The spontaneous emission was detected by a dielectric bandpass filter and a photomultiplier (temporal studies) while, for spectrally resolved measurements, the photomultiplier was replaced by a 0.6-m spectrograph operated in first order. This particular neutral Xe line was chosen for observation since it is known to be strongly fed by the dissociative recombination of Xe_2^+ ions.[15,16]

In summary, the experimental setup of Fig. 1 allows for simultaneously monitoring the electron and Xe* $6p$ densities in real time. Also, absolute electron densities are determined by first measuring the collision frequency for momentum transfer. There are several advantages in using this microwave detection scheme in photoionization experiments. One is that since a photoelectron is detected immediately upon being "created," these experiments are not confined to low pressures and electron densities ($<10^9-10^{10}$ cm^{-3}). The maximum electron density that can reliably be measured using a biased electrode configuration is constrained by space-charge effects. For the X-band microwave technique, cutoff of the waveguide places a ceiling of $\sim2\times10^{13}$ cm^{-3} on the measurable plasma density. For larger electron concentrations ($\gtrsim5\times10^{13}$ cm^{-3}), inverse bremsstrahlung involving an ir laser such as CO_2 has previously been shown to be useful.[17,18] Secondly, electron avalanche and excitation of the background gas are minimized.

III. EXPERIMENTAL RESULTS AND DISCUSSION

A. Xenon

Figure 2 shows the variation of the peak electron density with the ArF laser intensity for two different Xe pressures, 100 and 300 Torr.[19,20] The solid lines drawn through the data have a slope of 2 which confirms the quadratic intensity dependence of the two-photon ionization process. For both sets of data, however, deviation from quadrature is observed for $n \gtrsim 2\times10^{13}$ cm^{-3} which (as mentioned in

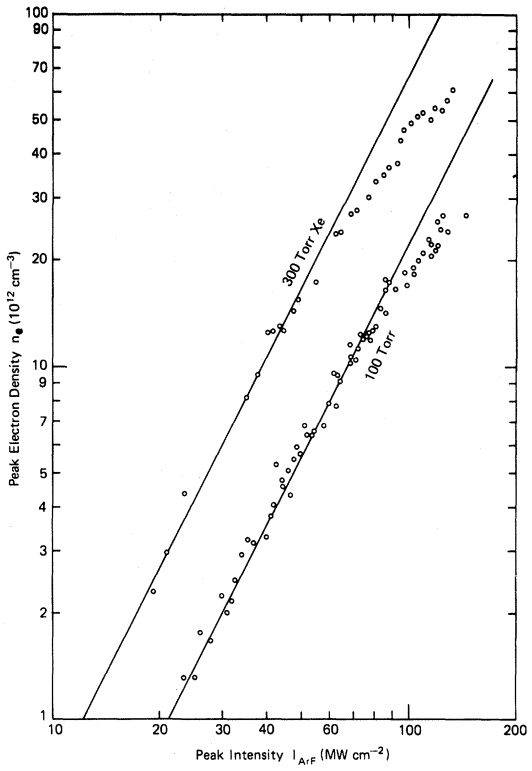

FIG. 2. Dependence of the photoelectron density on the ArF laser intensity at the focus. The solid lines have a slope of 2 which confirms the quadratic variation of the ionization rate with intensity.

TABLE I. Summary of the coefficients for two-photon ionization of xenon and propane at 193 nm (units of $cm^4 W^{-1}$).

Xenon			
Present work	Bischel *et al.*[a]	Hodges, Lee, and Moseley[b]	McGuire[c]
4×10^{-32}	1×10^{-34}	5×10^{-34}	8×10^{-32}
Propane			
Present work	Lee and Bischel[d]		
1.2×10^{-31}	3.0×10^{-31}		

[a]Reference 11.
[b]Reference 12.
[c]Reference 13.
[d]Reference 23.

Sec. II) is believed to be due to the onset of cutoff in the microwave system rather than saturation of the ionization mechanism itself. Also, for a given ArF intensity, the 300- and 100-Torr electron densities differ by almost a factor of 3 which one would also expect.

This I^2 dependence of the electron density was also observed (although not shown here) for Xe pressures as low as 10 Torr. (A 1-Torr tube was also prepared but the observed electron densities were too low to be reliably measured.)

The rate equation that describes the temporal behavior of the electron density is

$$\frac{dn}{dt}=\frac{\alpha[\mathrm{Xe}]I^2}{\hbar\omega}-\beta_1[\mathrm{Xe}^+]n-\beta_2[\mathrm{Xe}_2^+]n\ , \tag{9}$$

where [ ] denote particle concentrations, α is the two-photon ionization coefficient and has the units of $cm^4 W^{-1}$, β_1 and β_2 are the coefficients for recombination of electrons with Xe^+ and Xe_2^+ ions, respectively, and $\beta_1 \ll \beta_2$.[15]

The electron density is, however, experimentally observed to rise rapidly ($\sim$12-ns risetime for $p_{\mathrm{Xe}}=100$ Torr) and peak at the end of the ArF pulse. Subsequently, n decays slowly (e^{-1} time of ~1 μs for 100-Torr Xe). Therefore, the measurement of the peak electron density is made at a time at which few Xe^+ or Xe_2^+ ions have recombined. Consequently, the electronic recombination term in (9) can be ignored and the solution to the differential equation is simply

$$n=\frac{\alpha[\mathrm{Xe}]}{\hbar\omega}\int I^2dt\ . \tag{10}$$

Also in Eq. (10), depletion of the ground state is expected to be negligible.

Consequently, α was determined by time integrating the square of the time-resolved laser intensity (from photodiode waveforms) and, with a knowledge of the peak intensity (100 mJ of laser energy corresponds to 84 MW/cm^2 at the focus), using the data of Fig. 2. Over several trials, $\int I^2dt$ for a 100-mJ pulse was found to be 9.7×10^7 $W^2\,s\,cm^{-4}$.

A comparison of the value for α reported here with those published previously is given in Table I. Assuming a laser linewidth of 100 cm^{-1}, Bischel and co-workers[11] estimated α to be 1×10^{-34} $cm^4 W^{-1}$ and Hodges *et al.*[12] found 5×10^{-34} $cm^4 W^{-1}$ to be the lower limit for α. Bischel *et al.* did, however, point out that "... (autoionizing) resonances could enhance the value of α ... by a factor of 10^2."[11] As mentioned by Stebbings, Dunning, and Rundel,[21] the autoionizing states that have been observed in Xe are closely coupled to the ionization continuum, giving rise to broad autoionization peaks (on the order of 100 cm^{-1} width). Thus, despite the large linewidth of the ArF laser used in these experiments (140 cm^{-1}), it would seem to be well suited to exciting the $7d'[1\frac{1}{2}]$ ($J=2$) autoionizing state. It is expected to lie in close proximity to the $J=1$ state at 103 419 cm^{-1} which is 47 cm^{-1} from 103 466 cm^{-1} (twice the energy of ArF line center).

McGuire[13] has recently reported calculations of the two- and three-photon cross sections for ionization of the rare gases by circularly and linearly polarized radiation. Above 184.3 nm, σ is observed to drop rapidly [since $Xe^+(^2P_{1/2})$ can no longer be ionized by two photons] and σ (circular polarization) is found to be 8×10^{-32} $cm^4 W^{-1}$ at 193 nm. While the cross section for linear polarization is $\sim$20% lower than this value, both are within a factor of 2 of the result reported here.

In contrast to the recently observed four-photon ionization[8] of Xe (resonantly enhanced by the $7s[\frac{3}{2}]_1$ state), pressure effects are expected to have a negligible effect on the α reported here. There are

two reasons for this conclusion. One is that the ionization rate was observed to vary as I^2 for all the pressures studied and, as shown in Fig. 2, for a given intensity, the peak electron density was roughly linear in Xe pressure. Secondly, the first single-photon-allowed excited state in Xe is the $6s[\frac{3}{2}]_1$ level at 8.4 eV which is ~ 2 eV more energy than that of a single ArF photon. Therefore, near resonant atomic or molecular[22] interactions play a negligible role in the two-photon ionization process at 193 nm.

Hence, the values of α and ν_m presented here suggest that two-photon excitation of one or more autoionization states is occurring and that the products of ionization are a Xe^+ ($^2P_{3/2}$ core) ion and an electron of ~ 0.7-eV energy.

B. Propane

As a further check on the experimental and analytical procedures described earlier, the two-photon ionization of propane was also examined and the results compared with experiments recently completed by Lee and Bischel.[23] Using a different electron detection scheme, they determine α (C_3H_8) to be 3.0×10^{-31} cm^4 W^{-1}.

If electron attachment and recombination are, for the moment, ignored, then we find α to be 1.2×10^{-31} cm^4 W^{-1}. However, the temporal history of the electron density following ArF photoionization of propane indicates that (as pointed out by Lee and Bischel)[23] these two loss processes are significant. Specifically, for $p_{C_3H_8}=100$ Torr, the electron density is found to peak in less than 10 ns and exhibits an e^{-1} decay time of ~ 30 ns. Therefore, while the ionization coefficients of Ref. 23 and the present work are already in reasonable agreement, accounting for recombination and attachment will raise the latter number, thus bringing it into even better agreement with the value reported by Lee and Bischel.

IV. CONCLUSIONS

The two-photon ionization coefficient for Xe at 193 nm has been measured using a microwave bridge to obtain absolute electron densities. Although considerably larger than two previous estimates, the α reported here (4×10^{-32} cm^4 W^{-1}) is in agreement with the theoretical calculations of McGuire. Secondly, the two-photon coefficient for ionization of propane at the same wavelength was determined to be roughly within a factor of 2 of the number recently published by Lee and Bischel.

With the microwave bridge, ν_m is found to be consistent with an initial electron energy of 0.7 eV that is expected for this two-photon process. This measurement technique is versatile and readily applicable to a wide range of photoionization studies. Currently, it is being used to examine the three-photon ionization of Kr at 248 nm (KrF).

The measurement of α provides access to detailed and quantitative studies of the chemistry of Xe^+ or Xe_2^+ ions. Its application to examining the formation of ion clusters (Xe_n^+) and excimer molecules appears to be particularly promising.

ACKNOWLEDGMENTS

The authors wish to thank J. T. Verdeyen and J. T. Moseley for many interesting and helpful discussions on this subject and J. Reintjes for reviewing the manuscript. Also, the excellent technical assistance of Y. Moroz, K. Kuehl, and A. B. Wilson is appreciated. Finally, the support of this work by the National Science Foundation (R. E. Rostenbach) under Grant No. CPE 80-06378 is gratefully acknowledged.

[1]G. S. Voronov and N. B. Delone, Zh. Eksp. Teor. Fiz. 50, 78 (1966) [Sov. Phys.—JETP 23, 54 (1966)].

[2]T. M. Barhudarova, G. S. Voronov, G. A. Delone, N. B. Delone, and N. K. Martakova, in *Proceedings of the Eighth International Conference on Phenomena in Ionized Gases, Vienna, 1967* (Springer, Berlin, 1967), p. 266.

[3]P. Agostini, G. Barjot, J. F. Bonnal, G. Mainfray, C. Manus, and J. Morellec, IEEE J. Quantum. Electron. QE-4, 667 (1968).

[4]L. A. Lompre, G. Mainfray, C. Manus, and J. Thebault, Phys. Rev. A 15, 1604 (1977); see also P. Lambropoulos, Adv. At. Mol. Phys. 12, 87 (1976).

[5]S. E. Harris, A. H. Kung, E. A. Stappaerts, and J. F. Young, Appl. Phys. Lett. 23, 232 (1973).

[6]K. Aron and P. M. Johnson, J. Chem. Phys. 67, 5099 (1977).

[7]C. H. Chen, G. S. Hurst, and M. G. Payne, Chem. Phys. Lett. 75, 473 (1980).

[8]M. Rothschild, J. Zavelovich, W. Gornik, and C. K. Rhodes, Opt. Commun. 39, 316 (1981).

[9]J. C. Miller, R. N. Compton, M. G. Payne, and W. W.

Garrett, Phys. Rev. Lett. 45, 114 (1980); R. N. Compton, J. C. Miller, A. E. Carter, and P. Kruit, Chem. Phys. Lett. 71, 87 (1980); J. C. Miller and R. N. Compton, Phys. Rev. A 25, 2056 (1982).

[10]P. Agostini, F. Fabre, G. Mainfray, G. Petite, and N. K. Rahman, Phys. Rev. Lett. 42, 1127 (1979).

[11]W. K. Bischel, J. Bokor, D. J. Kligler, and C. K. Rhodes, IEEE J. Quantum Electron. QE-15, 380 (1979) and references cited therein.

[12]R. V. Hodges, L. C. Lee, and J. T. Moseley, Int. J. Mass Spectrom. Ion Phys. 39, 133 (1981).

[13]E. J. McGuire, Phys. Rev. A 24, 835 (1981).

[14]L. S. Frost and A. V. Phelps, Phys. Rev. 136, A1538 (1964).

[15]Y.-J. Shiu, M. A. Biondi, and D. P. Sipler, Phys. Rev. A 15, 494 (1977).

[16]For the Xe pressures and electron temperatures involved in these experiments, dissociative recombination of Xe_2^+ ions is the dominant electron loss process.

[17]E. Zamir, C. W. Werner, W. P. Lapatovich, and E. V. George, Appl. Phys. Lett. 27, 56 (1975).

[18]S. Alroy and W. H. Christiansen, Appl. Phys. Lett. 32, 607 (1978).

[19]The minimum detectable electron density in these experiments is $n \sim 4 \times 10^{11}$ cm^{-3}. Consequently, the discussion to follow will concentrate on the higher-pressure (and, thus, higher-n) data.

[20]Regardless of the care taken in cleaning a quartz cell, a detectable number of electrons are ejected from the cell walls due to the incident laser. For the highest ArF intensities, these electrons comprised $< 2\%$ of the total electron density and the data shown in Fig. 2 have been corrected for this effect.

[21]R. F. Stebbings, F. B. Dunning, and R. D. Rundel in *Atomic Physics 4,* edited by G. Zu Putlitz, E. W. Weber, and A. Winnacker (Plenum, New York, 1975), pp. 713–730.

[22]H. P. Grieneisen, K. Hohla, and K. L. Kompa, Opt. Commun. 37, 97 (1981).

[23]L. C. Lee and W. K. Bischel, J. Appl. Phys. 53, 203 (1982).